Fuel 134 (2014) 467–476

Contents lists available at ScienceDirect

Fuel

journal homepage: www.elsevier.com/locate/fuel

Investigation of heat of biomass pyrolysis and secondary reactions by simultaneous thermogravimetry and differential scanning calorimetry

Qun Chen [a,*], Ruiming Yang [a], Bo Zhao [a], Yan Li [a], Shujuan Wang [a], Hongwei Wu [b], Yuqun Zhuo [a], Changhe Chen [a]

[a] Key Laboratory for Thermal Science and Power Engineering of Ministry of Education, Department of Thermal Engineering, Tsinghua University, Beijing 100084, China
[b] School of Engineering, University of the West of Scotland, Paisley PA1 2BE, United Kingdom

HIGHLIGHTS

- TG–DSC technique was re-examined to determine the heat of biomass pyrolysis.
- Temperature-dependent specific heat was measured for biomass and char samples.
- The primary pyrolysis was found to consist of endothermic and exothermic stages.
- Linear relations were found between the biomass pyrolysis heat and conversion ratios.
- The heat of secondary reactions could be up to 2500–4000 J/g for the biomass samples.

ARTICLE INFO

Article history:
Received 16 July 2013
Received in revised form 7 May 2014
Accepted 29 May 2014
Available online 19 June 2014

Keywords:
Biomass pyrolysis
Heat of pyrolysis
Secondary reaction
Differential scanning calorimetry
Specific heat capacity

ABSTRACT

The heat of pyrolysis reactions is of great importance not only for its impact on biomass pyrolysis process but as a fundamental parameter for modelling biomass thermochemical conversion. Previously frequently-used technique that integrates DSC heat flow curves to determine the heat of pyrolysis actually presented the enthalpy change of pyrolysis within a temperature range. This enthalpy change in effect took no account of the sensible heat of the volatiles leaving the crucible before reaching the upper limit of the temperature range. This work was attempted to determine both the heat of biomass pyrolysis as a function of conversion ratios or temperatures and the heat of secondary reactions. To this end, the conventional simultaneous thermogravimetry (TG) and differential scanning calorimetry (DSC) technique was re-examined to investigate thermal behaviour of cellulose, xylan, lignin and four lignocellulosic biomass samples using a TG–DSC analyser. Selected samples around 3.3 mg were thermally decomposed in a crucible either with or without a pierced lid at a heating rate of 10 °C/min to a maximum temperature of 500 °C. Specific heat capacities of all the original biomass and char samples were measured through DSC analyses. Temperature-dependent formulas were developed for extrapolating the specific heat of both biomass and char samples at high temperatures. The heat of pyrolysis as a function of conversion ratios was characterised by the derivative of the enthalpy change versus mass changes during pyrolysis. Thus-obtained heat of biomass pyrolysis represented the difference between the enthalpies of formation of the products and reactants at a specific temperature or conversion ratio instead of a temperature range. The results showed that the heat of pyrolysis reactions changed from high endothermic values, via moderately endothermic values and finally rapidly to high exothermic values as the conversion ratios increased. Linear relations were established between the heat of biomass pyrolysis and conversion ratios ranging from 0.2 to 0.8. The heat of secondary reactions was about 80–280 J/g for cellulose and increased with conversion ratios up to 2500–4000 J/g for the lignocellulosic biomass samples.

1. Introduction

As the only carbon-based renewable energy resource, biomass is potentially more compatible with existing energy conversion and utilisation technologies than other renewables. Among various biomass conversion technologies, pyrolysis is one of the important and promising thermochemical conversion processes that can transform biomass into biofuels. Pyrolysis is also the primary and fundamental step to combustion and gasification. Consequently, there have been great research interests to achieve better

* Corresponding author. Tel.: +86 (0) 10 6279 3154; fax: +86 (0) 10 6277 5701.
E-mail address: qunchen@tsinghua.edu.cn (Q. Chen).

http://dx.doi.org/10.1016/j.fuel.2014.05.092
0016-2361/

Nomenclature

c_p	specific heat capacity (J/g K)
m	mass or weight (g)
$\dot{m}$	mass flow rate (g/s)
h	enthalpy (J/g)
q	heat per unit mass (J/g)
Q	heat (J)
Subscript	
b	unconverted biomass
c	char
DSC	DSC signal
e	end of the pyrolysis process
i	intermediate point
m	per unit mass change
t	time (s)
T	temperature (K)
Y	yield of products from biomass pyrolysis (%)
α	conversion ratio
β	heating rate (K/s)
γ	mass ratio of char to the initial sample
py	pyrolysis
rad	radiation
s	substance in the sample crucible
t	termination point
V	vapour products of biomass pyrolysis

understanding of biomass pyrolysis process in order for technology development and optimisation [1–3]. Among the various fundamental knowledge related to biomass pyrolysis, the heat of pyrolysis is one of the most important factors for reactor design, model simulation, process optimisation, and economic evaluation [3–6]. It is thus essential to quantitatively determine the thermal characteristics of biomass pyrolysis.

To date, there have been a number of studies investigating the heat of pyrolysis for biomass [4,6–11]. However, as the value of this quantity depends heavily on feedstocks, temperature ranges, the extent of secondary reactions among primary pyrolysis products and even on measurement conditions, accurate characterisation of the heat of pyrolysis is difficult [8]. Various inconsistent results have been reported ranging from endothermic to exothermic values. Some of these results were recently summarised in the literature [12]. Most studies on the heat of biomass pyrolysis have been carried out using differential scanning calorimetry (DSC) or simultaneous thermogravimetry (TG) and DSC [7,9–11]. DSC provides a convenient method for measuring quantitatively the heat flow to a sample as the temperature of the sample varies. The heat of pyrolysis is then determined by integrating the heat flow curves against time. Lee et al. [13] investigated wood pyrolysis process in laser radiation and calculated the heat of pyrolysis using obtained information of decomposition rates, temperature and pyrolysis gas compositions. The overall mass weighted endothermic heat of wood pyrolysis was about 610 J/g at low heat flux [12]. Most recently, Yang et al. [4] employed thermodynamic calculations to estimate the heat required for biomass pyrolysis in a screw-conveyor reactor after measuring the yields and composition for gaseous, volatile and char products.

However, it should be mentioned that most of the results reported in the literature were indeed the enthalpy change of biomass pyrolysis within a specified temperature range. These values indicated the energy released or required for biomass pyrolysis during this temperature range. Essentially, mathematical modelling for biomass pyrolysis prefers the heat of reaction as a function of temperature or conversion for solving energy conservation equations [3,12]. Still, to the best of the authors' knowledge, no such results for the heat of pyrolysis reactions have been reported so far. Therefore, the main objective of this study was to re-examine the TG–DSC technique and to characterise the heat of reactions with respect of the biomass pyrolysis process. The impacts of secondary reactions on the heat of pyrolysis were also investigated. These goals were achieved by conducting simultaneous TG–DSC tests for pyrolysis of seven selected biomass samples.

In order to determine the heat of pyrolysis reactions, specific heat capacities of both biomass feedstocks and their derived chars need to be specified. A few attempts have been made to measure the heat capacities of various biomass samples using DSC [14], adiabatic calorimetry [15] or the laser flash method [16]. Similar to the situations for the heat of pyrolysis, however, the reported heat capacity values for cellulose and wood samples were inconsistent among different studies. Moreover, even fewer studies have been conducted to measure the heat capacity of char derived from biomass pyrolysis. The specific heat of wood char was usually assumed to be that of graphite [17]. In this study, the heat capacities of biomass and char samples were carefully measured by TG–DSC analyses before biomass pyrolysis tests were carried out. The ratio method, a comparative technique, was used to determine the specific heat capacities of all the studied samples with powdery α-Al_2O_3 as a standard reference. This method could minimise the effects of thermal lag arising from variations in heating rates and sample sizes on the results [18].

2. Material and methods

2.1. Samples

Four lignocellulosic biomass feedstocks, including poplar wood chips, pine wood bark, corn stalk and rice straw, were selected for this study. These are commonly available forestry and agricultural residues in China and could potentially be used for massive biofuel production. All these biomass samples were ground to pass a 0.5 mm sieve. In addition, individual biomass constituents, namely cellulose (medium fibres, Sigma–Aldrich), hemicellulose (beechwood xylan, Sigma–Aldrich) and alkali lignin (Tokyo Chemical Industry Co., Ltd., Japan) samples were also used for comparison with the biomass samples. The fractions of the main components, the proximate and ultimate analyses of the samples are listed in Table 1. All these samples were oven-dried at 105 °C for 24 h.

99.99% pure aluminium oxide (α-Al_2O_3) was used as a standard material for heat capacity measurements. The aluminium oxide sample was heated to 1200 °C for 3 h before use. Some char samples were also prepared by heating above-mentioned biomass samples (5–10 g) loaded in 20 ml alumina crucibles with lids to 700 °C for 30 min in a muffle furnace. These char samples were used for c_p measurements and to characterise the radiation effect in TG–DSC tests (as mentioned in Section 2.2).

2.2. TG–DSC analyses for biomass pyrolysis and specific heat measurements

A Netzsch STA 449F3 thermal analyser (Fig. 1) was used for simultaneous TG–DSC measurements. Biomass pyrolysis tests

Table 1
Properties of the biomass samples.

Samples	1 Cellulose	2 Xylan	3 Alkali lignin	4 Poplar	5 Pine wood bark	6 Rice straw	7 Corn stalk
Proximate analysis (%, ad)							
Moisture	3.41	5.87	15.9	4.48	4.68	4.72	5.85
Volatile matter	94.4	78.5	62.3	80.3	68.6	70.8	75.3
Ash	–	3.47	13.63	1.49	13.52	12.86	7.72
Fixed carbon[a]	2.23	12.16	8.21	13.7	13.17	11.65	11.17
Ultimate analysis (%, daf)							
C	43.96	44.43	61.84	49.81	51.12	46.85	48.14
H	6.14	6.50	5.13	5.71	5.86	5.93	6.17
N	0.11	0.15	0.27	0.32	0.84	0.74	1.74
S	–	–	1.13	0.05	0.37	0.12	0.12
O[a]	49.79	48.92	31.63	44.09	41.81	46.36	43.84
Components (%, daf)							
Cellulose				35.91	35.35	40.99	36.43
Hemicellulose				17.07	15.91	24.52	26.48
Lignin				39.8	41.25	25.14	27.33
Extractive				3.18	3.53	5.16	6.73

[a] By difference.

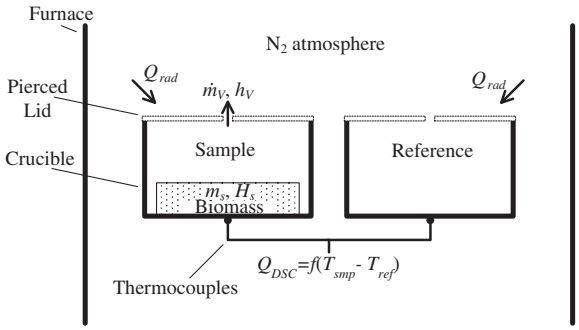

Fig. 1. Schematic diagram of the TG–DSC analyser.

were performed with highly pure nitrogen (purity > 99.999%) as purge gas. The flow rate of the nitrogen purge gas was 80 ml/min. In order to restrain sample size fluctuation from deteriorating reproducibility, the sample weights in all the experimental tests varied between 3.20 and 3.45 mg. Such sample weights offered to minimize probable thermal gradients and mass transfer limitations during pyrolysis without losing sample representation [1,2]. Two platinum crucibles were used as the sample and the reference holders respectively. The relative weight difference between these two crucibles was around 1%. The crucibles were used with or without pierced lids for the purpose of establishing different pyrolysis conditions. In the cases with lids, both the sample and the reference crucibles were topped by platinum covers, each with a 1 mm diameter hole in the centre.

At the beginning of each test, after a sample had been loaded in the sample crucible, the simultaneous TG–DSC analyser was equilibrated at 50 °C for 20 min. The furnace then heated the sample at a ramping rate of 10 °C/min up to 500 °C where the biomass sample was devolatilised to form char residue. Before each TG–DSC test for a biomass sample, baselines for simultaneous TG and DSC were obtained with empty crucibles following the identical temperature program as that of the sample. In order to analyse the radiation heat to the samples when the crucibles were used without lids, additional DSC curves were obtained by heating from 50 to 500 °C some beforehand prepared char samples (as mentioned in Section 2.1) in crucibles without lids in the TG–DSC analyser. All the TG and DSC curves were corrected by the baselines. All the tests were repeated for 2–3 times at least. Since the positioning of the sample crucible in the analyser and the thermal contact between sample and the holder could be slightly different each time, the repeatability of the DSC measurements was within 15% based on the repeated analyses.

In order to derive the heat of biomass pyrolysis from DSC curves, it is essential to measure the specific heat capacities of both the original biomass samples and their derived chars. Determination of the specific heat capacity for each virgin biomass or char sample was conducted according to the ratio method (ASTM E1269-11). DSC tests were performed in two Pt crucibles with pierced lids. The relative mass difference between these two holders was less than 0.5%. During the specific heat capacity measurements, 3.20–3.40 mg samples were used. Before the tests, the virgin biomass samples were all heated to 150 °C for 2 h and then kept in a desiccant for use. This ensured the moisture in the biomass samples was entirely removed while kept the main polymeric components unchanged. Inevitably, this pretreatment could lead to the decomposition of some extractives in the biomass samples. However, this may only exert minor effects on the specific heat capacities of the original biomass samples and thus be ignored. As the amount of char directly derived from biomass pyrolysis during a TG–DSC test was very small (about 0.2–1 mg), 3.20–3.40 mg char samples prepared beforehand (as mentioned in Section 2.1) were used for c_p measurements in order for improving the sensitivity and accuracy of DSC signals. The DSC test program for specific heat measurements was similar to that for biomass pyrolysis. Powdery α-Al_2O_3 was used as the standard sample for the specific heat capacity measurements and followed the same temperature programme for the DSC analysis. All the DSC curves were corrected with baselines obtained from runs with the empty crucibles prior to each sample test. All the analyses for the standard and biomass samples were repeated for 2–4 times. The repeatability was within ±10%. Correspondingly, the accuracy of c_p values was within ±14%.

2.3. Determination of the heat of pyrolysis

2.3.1. Mass balance for biomass pyrolysis

In order to derive the mass balance for biomass decomposition in the TG–DSC tests, a broad scheme as Eq. (1) is enough to describe the pyrolysis reactions. Taking m_0 as the initial mass of a biomass sample for a TG–DSC run, the mass conservation during the pyrolysis process could be expressed by Eq. (2),

$$\text{Biomass} \rightarrow \text{Char} + \text{Volatiles} + \text{Gases} \quad (1)$$

$$m_0 = m_s + m_V \tag{2}$$

where m_s is the mass of the substance left in the sample crucible and m_V is the mass of the pyrolysis vapours, i.e., the volatiles and permanent gases. Usually, a conversion ratio, α, can be defined to specify the progress of the pyrolysis reactions (Eq. (3)).

$$\alpha = \frac{m_0 - m_s}{m_0 - m_e} = \frac{m_V}{m_0 - m_e} \tag{3}$$

where m_e is the residual mass after the pyrolysis process. As α approaches 1, the pyrolysis process of the biomass sample comes to an end for the TG–DSC test. All the virgin biomass particles turn to be char. Thus, the mass ratio of char to the initial sample can be determined by $\gamma_c = m_e/m_0$. In other words, the amount of the pyrolysis vapours and that of the residual char have the following relation (Eq. (4)),

$$\frac{m_0 - m_e}{m_e} = \frac{1 - \gamma_c}{\gamma_c} \tag{4}$$

In order to estimate the specific heat capacity of the sample in the crucible during pyrolysis, m_s in Eq. (2) could be assumed as the mass of char and unconverted biomass particles (with masses of m_c and m_b, respectively), i.e.,

$$m_s = m_c + m_b \tag{5}$$

Although Agarwal and Lattimer [19] employed such an assumption in measuring the heat of decomposition of charring materials, this assumption would be more appropriate if the particle size or the quantity of the biomass sample was large. In the case of small particle size and sample quantity, the suitability of this assumption in c_p calculation should be verified. It is convenient to assume that the mass ratio of pyrolysis vapours to char still follows Eq. (4) during the pyrolysis process. From Eqs. (2) and (5), Eq. (4) can be rewritten as,

$$\frac{m_V}{m_c} = \frac{1 - \gamma_c}{\gamma_c} \tag{6}$$

With Eq. (6), the mass of char produced during the biomass pyrolysis process, m_c, can then be estimated as,

$$m_c = \frac{\alpha\gamma_c(m_0 - m_e)}{1 - \gamma_c} \tag{7}$$

The amount of unconverted biomass, m_b, could be calculated as,

$$m_b = m_0 - \frac{\alpha(m_0 - m_e)}{1 - \gamma_c} \tag{8}$$

As m_0, m_e, and m_s can be obtained from a TG curve, once the specific heat capacities of the original biomass and the residual char ($c_{p,b}$ and $c_{p,c}$ respectively) are obtained, the heat capacity of the biomass sample during the pyrolysis process ($c_{p,s}$) could be deduced by,

$$c_{p,s} = \frac{1}{m_s}\left(m_b c_{p,b} + m_c c_{p,c}\right) \tag{9}$$

Eq. (9) provides a linear approximation with respect to the conversion ratio, α. for the $c_{p,s}$ determination.

To verify the validation of Eqs. (5) and (9), additional c_p measurements were carried out for chars derived from pyrolysis of the rice straw (#6 in Table 1) at different stages of conversion. The measurement procedure followed that described in Section 2.2. The measured c_p values were compared with those calculated according to Eq. (9).

2.3.2. Heat of biomass pyrolysis

As DSC data corrected with baselines generally give out heat flow rates to samples in TG–DSC analyses, the energy balance could therefore be formulated as [18,19],

$$\frac{dQ_{DSC}}{dt} = \frac{d(m_s h_s)}{dt} + \dot{m}_V h_V + \frac{dQ_{rad}}{dt} \tag{10}$$

for an open crucible where biomass pyrolysis takes place, where Q_{DSC} is heat derived from DSC curves, h_s is the enthalpy of biomass sample, h_V is the enthalpy of the volatiles, $\dot{m}_V$ is the mass flow of the volatiles, Q_{rad} is the radiation heat from surrounding, as depicted in Fig. 1. In the cases where the crucibles are covered with pierced lids, the third item in the right-hand-side (RHS) vanishes.

Following Eq. (5), the first item in the RHS of Eq. (10) can be expanded as,

$$\begin{aligned}\frac{d(m_s h_s)}{dt} &= \frac{d(m_b h_b + m_c h_c)}{dt} \\ &= (m_b c_{p,b} + m_c c_{p,c})\frac{dT}{dt} + \frac{dm_b}{dt}h_b + \frac{dm_c}{dt}h_c\end{aligned} \tag{11}$$

Considering Eqs. (9), (10) can then be written as,

$$\frac{dQ_{DSC}}{dt} = m_s c_{p,s}\frac{dT}{dt} + \left(\frac{dm_b}{dt}h_b + \frac{dm_c}{dt}h_c + \dot{m}_V h_V\right) + \frac{dQ_{rad}}{dt} \tag{12}$$

As the volatiles and gases are leaving the crucible, $\dot{m}_V$ should be negative in value. The sums in the parentheses turn out to be the heat of pyrolysis [19] for the overall reaction shown by Eq. (1). Therefore, the heat of pyrolysis per initial sample mass, q_{py}, could be derived from DSC signals as follows [19].

$$\frac{dq_{py}}{dt} = \frac{dQ_{py}}{m_0 dt} = \frac{1}{m_0}\left(\frac{dQ_{DSC}}{dt} - m_s c_{p,s}\frac{dT}{dt} - \frac{dQ_{rad}}{dt}\right) \tag{13}$$

Substituting the heating rate $\beta = dT/dt$ into Eq. (13), the enthalpy change of pyrolysis between temperature T_1 and T_2 would be,

$$\Delta q_{py} = \frac{\Delta Q_{py}}{m_0} = \frac{1}{m_0\beta}\int_{T_1}^{T_2}\left(\frac{dQ_{DSC}}{dt} - m_s c_{p,s}\frac{dT}{dt} - \frac{dQ_{rad}}{dt}\right)dT \tag{14}$$

As a matter of fact, the heat of biomass pyrolysis that has often been reported in the existing literature was mostly thus defined (Δq_{py}) [6,9,11]. It should be stressed that, in a TG–DSC test, the volatiles escape the sample crucible soon after they are formed during biomass pyrolysis. Under this circumstance, the enthalpy change obtained by the integration from T_1 and T_2, as shown in Eq. (14), is unlikely to include the sensible heat of all the volatiles up to the final temperature T_2.

In this paper, the heat of reactions for biomass pyrolysis ($q_{m,py}$) is defined by the differentiation method as follows,

$$q_{m,py}(T) = \frac{dQ_{py}}{dm} \tag{15}$$

It is the heat of pyrolysis per unit mass change, essentially the difference between the enthalpies of formation of the products and reactants at any temperature or conversion ratio. This quantity is more useful than the enthalpy change of pyrolysis, Δq_{py}, in mathematical modelling of biomass pyrolysis [12]. It is worth noting that the radiative heat effect, Q_{rad} in Eqs. (12)–(14), should only be considered when the crucibles are without pierced lids in the TG–DSC tests.

3. Results and discussion

3.1. Specific heat capacities for biomass and char samples

As can be seen in Eqs. (9) and (13), the values of c_p for both virgin biomass and residual char samples were requisites for investigating the heat of biomass pyrolysis. In this study, the ratio method was employed to measure c_p through TG–DSC analyses. It should be noted that this method requires neither chemical reactions nor weight changes involved during the heating process (ASTM E1269-11). When heated over 180–200 °C, some biomass samples (such as the xylan and alkali lignin) began to decompose. Hence, the DSC data above 180–200 °C should not be used for biomass c_p analysis. Although the TG–DSC runs started from 50 °C after 20 min equilibrium period, there existed a transient stage for the samples before their actual temperature ramping rate reached 10 °C/min. During the transient period, the baselines were usually unstable. For the biomass samples, therefore, only DSC data between 70 and 200 °C were used for c_p calculation. In this study, seven char samples derived from biomass devolatilisation at 700 °C were used for c_p measurements. It was supposed that secondary decomposition could be negligible for these char samples at temperature below 500 °C. However, TG curves showed that the weights of the char samples began to decline very gently over 250 °C. Such decline could be easily overlooked unless the DSC curves were crosschecked, which showed marked changes in slope near 250 °C. As a result, for the char samples, DSC signals between 70 and 250 °C were used for c_p calculation.

Fig. 2 presents the measured c_p values for all the biomass and char samples. As can be seen in Fig. 2a, at 70 °C c.a., the c_p values were around 1.250–1.44 J/g K for all the dry biomass samples. The values of c_p increased almost linearly with temperature and varied between 1.75 and 2.13 J/g K around 200 °C. c_p values for the corn stalk (#7) were the highest among all the lignocellulosic biomass samples. However, the maximum relative difference among c_p values of all biomass samples were within 20%, only 1.5 times as much as the measurement accuracy limit, 14%, as mentioned in Section 2.2. In this sense, the differences among the c_p values for all these biomass samples were minor.

As shown in Fig. 2b, c_p values for the char samples were lower than their original biomass samples. It is interesting to note that the c_p values for the bark (#5), rice straw (#6) and corn stalk (#7) char samples were distinctly higher than those of cellulose (#1) and xylan (#2) whereas c_p of char derived from the poplar (#4) lay in between. The difference in c_p values among the char samples could be related to their ash contents in the original feedstocks. As can be seen in Table 1, the pine wood bark had the highest content of inorganic mineral matter, whereas the ash contents in the rice straw and corn stalk were higher than in the poplar sample. Pearson's correlation between cp values for char samples at 70–80 °C and the ash contents in the biomass samples varied around 0.68–0.76, with p-value of 0.04–0.09.

Fig. 2 also presents reported c_p values that were derived from some temperature-dependent relations in the literature. There were several empirical formulas for c_p of various wood samples in terms of temperature, as listed in Table 2. It is obvious that the c_p values obtained in this study agreed well with the reported specific heat of dry wood. For instance, both Rath et al. [9] and Gomez et al. [11] employed a linear temperature-dependent relation for heat capacity ($c_p = 1113.68 + 4.8567(T-273.15)$ (J/kg K)) in their studies for the heat of wood pyrolysis. As shown by the dashed line in Fig. 2, the c_p values calculated from this equation was very close to those of the corn stalk (#7). Although Comesana et al. [14] also used DSC analysis to measure biomass c_p and their results were close to this study below 100 °C, their c_p values increased sharply with temperature and showed much larger results. This discrepancy may be due to the method employed for c_p determination. They calculated the heat capacities on the basis of subtracting the sensible and latent heat of moisture evaporation from the absolute values of heat exchange derived from DSC curves [14]. Moreover, higher heating rate (30 K/min) and larger sample size (~20 mg) were used for DSC analyses in their study. Large sample size and fast heating rate usually lead to poor thermal equilibrium in DSC tests [18].

Very few data were available in the literature for verifying the obtained c_p values of char in this study. Specific heat of graphite has previously been used for wood char [17,21]. As illustrated in Fig. 2b, c_p values of graphite were very close to those of cellulose (#1) obtained in this study. Hansson et al. [22] reported a temperature dependent relation of c_p for wood chars. The c_p values calculated from this relation fell within the range of c_p values measured in this study. Rath et al. [9] calculated the c_p of wood char samples using an equation which was originally derived for coal char [23]. As shown in Fig. 2b, however, c_p values calculated from that equation were significantly higher than those obtained in this study. It should be mentioned that char samples obtained for c_p measurement in this study were the products of devolatilisation in a muffle oven at 700 °C. The effects of pyrolysis conditions on c_p values of biomass char requires further investigation.

Table 2 lists the temperature-dependent c_p relations obtained in this study by fitting the data in Fig. 2. These equations were extrapolated to 500 °C in order to quantify c_p values of biomass during pyrolysis based on Eq. (9).

Fig. 3 compares the calculated cp values based on Eq. (9) with measured cp values of rice straw chars obtained at conversions of 0.13, 0.31,0.65, and 0.92. The char samples were obtained from pyrolysis of the rice straw sample in the TG–DSC analyser with a heating rate of 10 K/min. The conversions were calculated

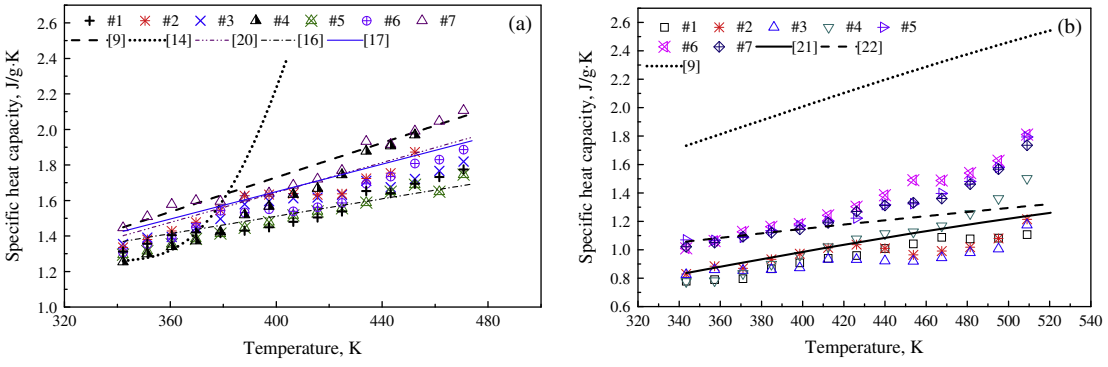

Fig. 2. Specific heat capacities for the biomass (a) and char (b) samples.

Table 2
Fitted temperature-dependent specific heat relations for the biomass and char samples.

Sample	Specific heat for biomass, J/kg K	R^2	Specific heat for char, J/kg K	R^2
#1	3.45 T + 118.94	0.940	2.23 T + 3.84	0.936
[24][a]	970 + 5.13(T–273)			
#2	4.09 T – 37.87	0.947	1.45 T + 370.98	0.705
#3	3.35 T + 222.62	0.972	0.99 T + 497.69	0.737
#4	6.14 T – 849.16	0.973	3.72 T – 529.38	0.974
[20][b]	4.206 T – 37.7			
[16][b]	2.45 T + 531.2			
[17][b]	3.867 T + 103.1			
#5	3.50 T + 89.68	0.988	3.23 T – 100.01	0.927
#6	4.21 T – 124.27	0.954	3.96 T – 361.87	0.979
#7	4.92 T – 258.65	0.940	3.14 T – 77.72	0.968

[a] Reported specific heat of cellulose.
[b] Specific heat of dry wood in the literature.

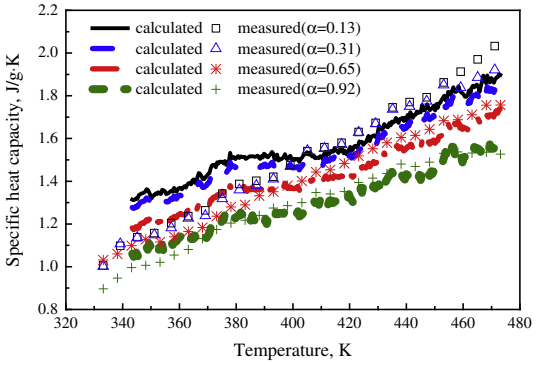

Fig. 3. Measured and calculated specific heat capacities of the rice straw chars at different stages of conversion.

according to Eq. (3). As shown in Fig. 3, the specific heat values of chars decrease with the increasing conversions. The calculated specific heat capacities of chars agree well (maximum difference within 10%) with those measured in the temperature range of 400–470 K. The calculated c_p values are greater than those measured between 340 and 400 K. The maximum difference is approximately 20% relative to the measured values. This implies that Eq. (9) can be used to estimate the specific heat of chars during pyrolysis within the accuracy of c_p measurement.

3.2. Results of TG–DSC analyses

Fig. 4a shows the representative TG–DSC results obtained from poplar wood pyrolysis with and without a pierced lid in this study. As expected, the TG curves demonstrated that the biomass pyrolysis proceeded through a primary decomposition stage (curve section "A" in Fig. 4a) followed by secondary thermolysis (curve section "B" in Fig. 4a) at temperatures exceeding 400 °C. During the primary pyrolysis stage, biomass was thermally degraded to form bulk of volatile matter and primary char residue. The char residue was then slowly subject to aromatisation and dehydrogenation in the secondary pyrolysis phase [2,9,25]. This study only concentrated on the thermal behaviour during the primary pyrolysis stage.

A termination temperature (T_t) of the primary pyrolysis stage could be determined from a TG curve. To specify the termination temperature, an extrapolated end point for curve "A" (the primary pyrolysis process) was first obtained from the intersection of the tangent at the inflection point of "A" with the right tangent baseline at curve "B". T_t was then determined on the TG curve where the weight loss was equal to that of the extrapolated end point. The values of T_t, as listed in Table 3, varied with different biomass samples and pyrolysis conditions.

The presence or absence of the pierced lids on the crucibles in TG–DSC tests affected not only T_t but also the yields of char and DSC curves. As can be seen in Fig. 4a, the char yield in the TG–DSC run with lids was slightly higher than that from the case without lids. When biomass pyrolysis takes place in a crucible with a lid, the primary volatiles would first be trapped in the crucible and thus enhance secondary char formation reactions. In an open crucible, however, the released volatile matter could readily diffuse into the purge gas stream. The partial pressure of the volatiles around the primary char surface remains low and more refractory components could decompose, leading to higher termination temperature (T_t) and lower char yields in the tests without lids.

Heat flow curves were more profoundly influenced by the lids on the crucibles. In the case with pierced lids, as shown in Fig. 4a, the DSC curve showed a slight slope relative to a flat

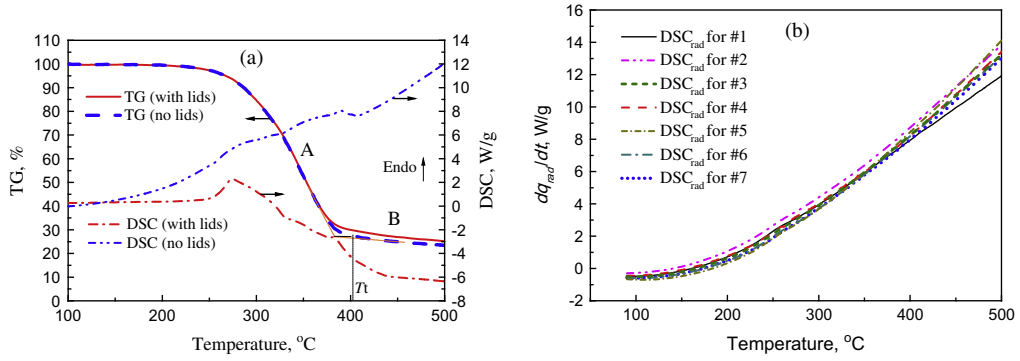

Fig. 4. (a) TG–DSC results for the poplar wood sample (#4) and (b) radiative heat flow curves for the biomass char samples.

Table 3
Summary of the results obtained from TG–DSC analyses.

Sample	Case	T_i °C	T_t °C	α_i %	α_t %	Δq_i J/g	Δq_t J/g	$Y_{c,t}$ %
1	With lids	363	383	79.1	96.2	313.8	143.2	12.9
	Without lids	377	396	86.7	96.9	426.3	261.6	10.5
2	With lids	–	330	–	77.6	–	−540.1	46.8
	Without lids	–	346	–	83.2	–	−169.3	46.4
3	With lids	–	440	–	89.7	–	−357.9	70.9
	Without lids	–	440	–	90.6	–	−203.3	70.8
4	With lids	313	392	28.9	92.6	332	−545.2	30.7
	Without lids	366	405	78.1	95.2	365.9	254.2	27.1
5	With lids	299	376	20.4	83.8	52	−911	49.4
	Without lids	345	379	52.9	84.7	110.8	−93.7	49.8
6	With lids	303	365	34.8	83.8	73.2	−889.4	47.7
	Without lids	322	368	51.6	86.4	132.6	−113.6	46.1
7	With lids	310	376	56.8	86.8	89.7	−532.1	43.6
	Without lids	352	387	73.4	89.9	164	58.8	41.3

baseline before 200 °C, reflecting changes in the specific heat of the poplar wood sample. As the pyrolysis process proceeded, an endothermic peak appeared around 270 °C and then the curve went downward to exothermic. In the case without lids, however, the DSC curve differed significantly from that of the case with lids as the baseline bended to endothermic side with the increasing temperatures due to the radiative heat effects [9,26]. In order to determine the reaction heat for pyrolysis for the cases without lids, therefore, the heat of radiation should be subtracted from the heat flow curve [9].

In this study, the radiative heat effect was determined by comparing DSC curves obtained from heating various char samples in the crucibles without lids to those obtained from the cases in the presence of lids. As shown in Fig. 4b, the DSC curves for the radiative heat flow for some biomass char samples were quite close although some discrepancy was observed on account of difference in char emissivity or TG–DSC test errors. These curves were used to correct the DSC results of biomass pyrolysis in the cases without lids following Eq. (13).

3.3. Heat of pyrolysis reactions

Fig. 5 presents the typical heat flow curves required to calculate the heat of pyrolysis, which were obtained from pyrolysis of the pinewood bark (sample #5) through TG–DSC tests. Together with these heat flow curves, DTG curves are also shown in Fig. 5. Due to the small sample sizes in the tests, only some minor differences could be observed between the DTG curve from the case with lids and that without lids.

Unlike the DTG curves, the corrected heat flow curves showed much marked differences reflecting the effects of the lid presence. The thermal behaviour of the process is a result of the competition between endothermic and exothermic reactions. In a lid-covered crucible, the volatiles produced from biomass pyrolysis take longer time to diffuse out of the crucible than in an open crucible, which leads to more secondary reactions of these vapour products with solid residue. Usually, these secondary reactions are exothermic [9,11]. As shown in Fig. 5, both heat flow curves indicated that the pyrolysis process was dominated by endothermic reactions after the pyrolysis began. In the tests without lids, secondary reactions were less severe since the released volatiles could diffuse more quickly out of the crucible. After passing the maximum endothermic peak around 300 °C, the heat flow curve gradually declined to exothermic at 345 °C. This trend of the heat flow curves was also observed by Milosavljevic et al. [8] in the pyrolysis process of cellulose at low heating rates. As the change from endothermic to exothermic stage occurred during the primary pyrolysis, the transition point was designated as an intermediate point with a temperature, T_i, in this study. Table 3 lists the intermediate temperatures and the corresponding conversion ratios (α_i) for all the biomass samples. However, as the pyrolysis of the lignin and xylan samples was exothermic from the beginning, no intermediate temperatures were attempted.

Based on Eq. (14), the enthalpy change of pyrolysis could be obtained by integrating the corrected heat flow curves from 200 °C to a specified final temperature, such as the intermediate temperature (T_i) and the termination temperature (T_t). These results are summarised in Table 3. Positive values of the enthalpy changes indicated endothermic reactions dominant in the corresponding temperature ranges. Considering the uncertainties in DSC measurements as mentioned in Section 2.2, the accuracy of derived enthalpy was estimated to be within ±26%.

It has been generally acknowledged that the cellulose pyrolysis is endothermic whereas the pyrolysis of hemicellulose and lignin are exothermic during the primary pyrolysis stage [27]. As the cellulose sample was medium fibres, the enthalpy change of cellulose pyrolysis obtained in this study was a bit higher than that of cellulose from Whatman filter paper (230 J/g) [7]. Stenseng et al. [10] measured the heat of pyrolysis for Sigma cellulose to be 450 J/g, which was close to Δq_i (426 J/g) shown in Table 3. The enthalpy change of pyrolysis for the poplar wood agreed well with those reported by Rath et al. [9] and Gomez et al. [11] Very few results have so far been published concerning the enthalpy change of pyrolysis for wood bark and agricultural residues. Gomez et al. [11] found the heat of pyrolysis for an untreated thistle crop to be −132.7 J/g. This value was close to those measured for the wood bark and rice straw (samples #5 and 6) in this study. Recently, Yang et al. [4] estimated the heat required for biomass pyrolysis in a screw-conveyor reaction at 500–550 °C to be 1100–1600 J/g. It should be stressed that these values were obtained from the enthalpy difference between all the products at the final temperatures and the biomass feedstocks at 25 °C. In a TG–DSC test,

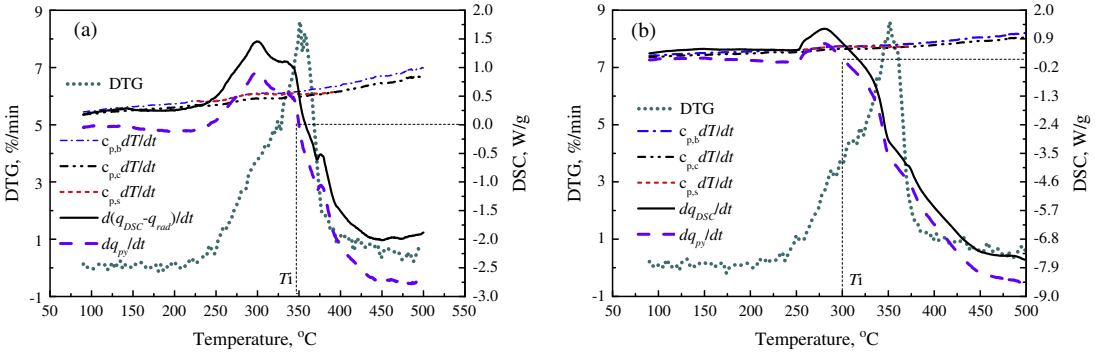

Fig. 5. DTG and DSC curves for the pinewood bark sample decomposed (a) without lids and (b) with lids.

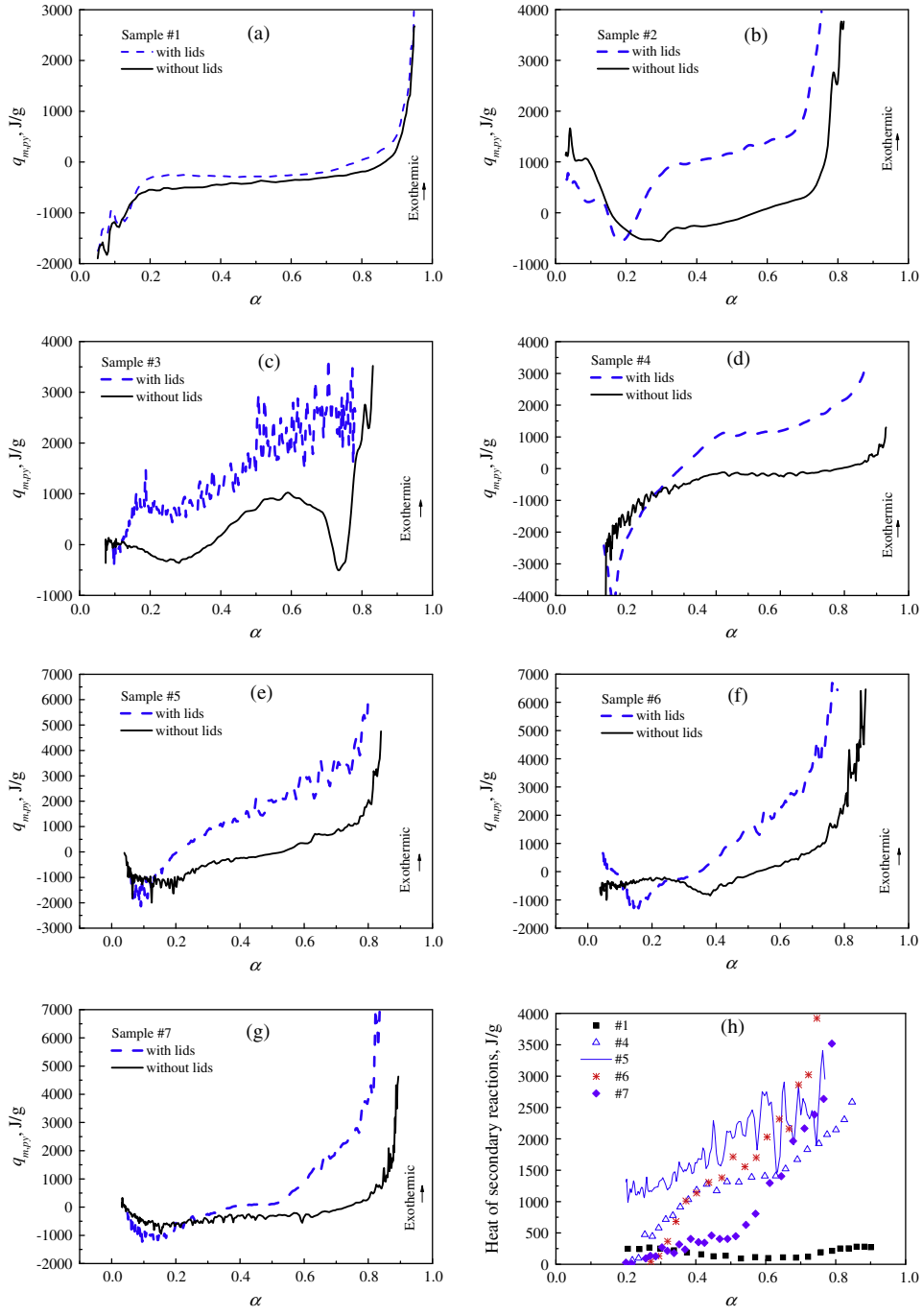

Fig. 6. Heat of pyrolysis (a–g) and secondary reactions (h) versus conversion ratios for the biomass samples.

Table 4
Relationships between the heat of pyrolysis reactions and conversion ratios for some biomass samples.

Samples	Heat of pyrolysis, $q_{m,py}$, J/g	Range of conversion ratios
1	541.0 α – 670.5	0.20–0.80
2	1727.1 α – 953.3	0.20–0.73
4	1096.1 α – 817.4	0.20–0.85
5	3532.4 α – 1690.9	0.20–0.80
6	3928.2 α – 2065.8	0.30–0.75
7	1076.0 α – 812.0	0.20–0.80

however, the primary volatiles escaped the sample crucible before the final pyrolysis temperature was reached. The enthalpy change of biomass pyrolysis obtained through Eq. (14) thus took into account only part of the sensible heat of the pyrolysis products when integrating the heat flow curves.

As listed in Table 3, the enthalpy changes of pyrolysis obtained from the cases with lids were lower than those obtained in the cases without lids. This manifested the exothermic effect of secondary reactions brought about with the presence of lids for crucibles in the TG–DSC tests. The magnitude of enthalpy change of biomass pyrolysis, Δq_t, for the wood bark and agricultural residues were much higher when compared with the results reported in the literature [11]. This was consistent with higher yields of char obtained by the end of primary pyrolysis for the wood bark and agricultural residues in this study.

It should be noted that the negative Δq_t values did not necessarily mean the whole primary pyrolysis to be exothermic for these biomass samples. The positive Δq_i showed quite endothermic pyrolysis reactions before reaching the intermediate temperatures. This implies that the integral values for the enthalpy change of pyrolysis, Δq_i and Δq_t, could only be used to estimate energy release or requirement for biomass pyrolysis. However, neither could reveal the evolution of the heat of pyrolysis reaction along the pyrolysis process. The revelation could be fulfilled through the heat of pyrolysis per unit mass change, $q_{m,py}$, calculated by Eq. (15).

Fig. 6 shows the evolution of heat of pyrolysis reactions per unit mass change with respect to conversion ratios during the primary pyrolysis for all the biomass samples. In contrast to the enthalpy change of pyrolysis per unit initial mass (Δq), the negative values of the heat of pyrolysis reactions were used for endothermic reactions, as shown in Fig. 6(a–g). In the cases without lids, the heat of pyrolysis reactions, $q_{m,py}$, altered from high endothermic values at the beginning, via relatively constant or steadily changed endothermic values, to high exothermic values towards the end of the primary pyrolysis. This tendency was also observed for $q_{m,py}$ values in the cases with lids. However, since $q_{m,py}$ was calculated by differentiation following Eq. (15), its values could be more susceptible to errors in mass changes. The influence of these errors on $q_{m,py}$ could be significant especially at the beginning and the end of the primary pyrolysis where the mass change rates (DTG) were low. Table 4 shows the fitted relationships between the values of $q_{m,py}$ obtained from the cases without lids and conversion ratios ranging roughly from 0.2 to 0.8.

As expected, due to the more likely secondary reactions, $q_{m,py}$ in the cases with lids was more exothermic than that obtained in the cases without lids over a wide range of conversion ratios. However, it is interesting to note that the $q_{m,py}$ values in the cases with lids were a bit lower than those in the cases without lids at the early stage of primary pyrolysis($\alpha < 0.2$). This may be explained as follows. In a TG–DSC test for biomass pyrolysis, the volatile products would accumulate in the sample crucible when the crucible was covered with a lid. These products would also absorb heat during the programed heating process. This portion of sensible heat was included into the heat of pyrolysis in Eq. (13). However, the amount of the sensible heat could only be accurately determined unless the composition of the evolved volatiles was fully disclosed.

Intuitively, the heat of secondary reactions could be determined by subtraction of the pyrolysis reaction heat for the cases without lids from that for the cases with lids. Fig. 6h shows thus-obtained heat of secondary reactions with respect to conversion ratios ranging from 0.2 to 0.8 for some biomass samples. As can be seen, the values of heat of secondary reactions were relatively low for the pure cellulose sample, varying between 80 and 280 J/g. For the lignocellulosic biomass samples derived from forestry and agricultural residues, however, the heat of secondary reactions increased with the conversion ratios up to 2500–4000 J/g. In addition to the cellulosic component, these biomass samples also consisted of more complex constituents, such as hemicellulose, lignin, and inorganic minerals. These components generally favour the formation of either primary or secondary char during biomass pyrolysis [28]. For this reason, the heat of secondary reactions for these composite biomass samples was higher than the pure cellulose sample. In the literature, the heat of char formation was usually obtained by linear regression fitting among the overall enthalpy change of the whole primary pyrolysis process versus final char yields. However, the reported values were inconsistent, varying from 2 kJ/g [10] to 3.6 kJ/g [29] and 3.8 kJ/g [9]. Although secondary reactions usually include both homogeneous and heterogeneous reactions leading to char formation, the heat of secondary reactions at high conversion ratios in this study appeared close to these reported values.

3.4. Influencing factors to the heat of pyrolysis

The heat of biomass pyrolysis could be influenced by various factors. For example, higher heating rates could lead to more condensable volatiles and permanent gases [28], which may change the total enthalpy of products and thus the heat of pyrolysis. However, the results reported by Yang et al. showed only 10% increment in the enthalpy change of pyrolysis reactions for a cedar sample when the heating rates increased from 32 to 320 °C/min. In this study, no attempt was made to investigate the effects of heating rate on the heat of pyrolysis reactions.

The main factors affecting the heat of biomass pyrolysis could be its main constituents (hemicellulose, cellulose, and lignin) and inorganic mineral matter. It was demonstrated that the weight loss during biomass pyrolysis and product distribution could roughly be expressed by linearly summative correlations of those obtained from the pyrolysis of three main constituents [30,31]. This conclusion was based on the results from biomass pyrolysis through TG analyses or packed-bed reactors where no significant interaction among these constituents was detected [30,31]. As far as the heat of pyrolysis is concerned, however, this kind of linearly summative relationship seems no longer valid between the composite biomass samples and individual constituents. Although homolysis of cross-linked structure and cleavage of relatively weak bonds in lignin may hardly change the pyrolysis behaviour in terms of weight loss, these reactions may be coupled with bond scission and dehydration reactions of cellulose. This could give rise to remarkable changes in the heat flow curves. Nonetheless, this inference needs to be checked by further investigation. On the other hand, inorganic mineral matter in the lignocellulosic biomass could also have impacts on the thermal behaviour of pyrolysis. As listed in Table 3, Δq_t appeared to decrease as the ash content in the biomass samples increased for both the cases without and with lids. This tendency was anticipated as the mineral matter could promote char-forming secondary reactions [2]. However, as this result was obtained from only a few biomass samples in this study, this effect of mineral matter on the heat of pyrolysis should be further investigated.

4. Conclusions

There have been some inconsistent results concerning the heat of pyrolysis reactions and the specific heat of biomass in the existing literature. Most previously reported enthalpy change of pyrolysis (Δq) within a specified temperature range did not consider the sensible heat of volatile products escaping the crucible before reaching the upper limit of the temperature range. In this paper, thermal characteristics during the primary pyrolysis process were studied for several forestry and agricultural residues, as well as for three individual biomass constituents using a TG–DSC analyser. The specific heat capacities of both original biomass feedstocks and chars were measured by the ratio method and were used to verify the existing data. The obtained heat capacities for biomass samples agreed well with some of the existing temperature dependent relations. The specific heat (c_p) values of biomass char samples were generally lower than those of original biomass. Chars derived from biomass with higher ash content appeared to have relatively higher specific heat values. These data were used for extrapolating the specific heat of both biomass and char samples at high temperatures for subsequent determination of heat of pyrolysis.

By means of differentiating the enthalpy change with respect to mass, the heat of pyrolysis for biomass, $q_{m,py}$, was characterised as a function of conversion ratios. Such heat of pyrolysis represents the difference between the enthalpies of formation of the products and reactants at a specific temperature even without the knowledge of product composition in detail. $q_{m,py}$ changed from high endothermic values to a moderately endothermic values and then rapidly to high exothermic values as the conversion ratios increased. The heat of secondary reactions was determined to be 80–280 J/g for cellulose and to increase with conversion ratios up to 2500–4000 J/g for the forestry and agricultural residues. These results could be used as fundamental data for solving energy conservation equations in biomass thermochemical conversion modelling.

No summative correlations for the heat of pyrolysis were found between three major biomass constituents and the selected lignocellulosic biomass samples. Although Δq_t was found roughly negatively correlated to the ash content in biomass, this effect of inorganic mineral matter needs further investigation.

Acknowledgements

This research work was financially supported by the National Natural Science Foundation of China (No. 51276099) and Tsinghua University Initiative Scientific Research Program (No. 2011Z02147). The authors would also like to thank the Laboratory Fund of Tsinghua University (LF20125120) for partial grant support.

References

[1] Antal MJ, Varhegyi G. Cellulose pyrolysis kinetics: the current state of knowledge. Ind Eng Chem Res 1995;34:703–17.
[2] White JE, Catallo WJ, Legendre BL. Biomass pyrolysis kinetics: a comparative critical review with relevant agricultural residue case studies. J Anal Appl Pyrolysis 2011;91:1–33.
[3] Di Blasi C. Modeling chemical and physical processes of wood and biomass pyrolysis. Prog Energy Combust Sci 2008;34:47–90.
[4] Yang H, Kudo S, Kuo H, Norinaga K, Mori A, Masek O, et al. Estimation of enthalpy of bio-oil vapor and heat required for pyrolysis of biomass. Energy Fuels 2013;27:2675–86.
[5] Park WC, Atreya A, Baum HR. Determination of pyrolysis temperature for charring materials. Proc Combust Inst 2009;32:2471–9.
[6] He F, Yi W, Bai X. Investigation on caloric requirement of biomass pyrolysis using TG–DSC analyser. Energy Convers Manage 2006;47:2461–9.
[7] Beall FC. Differential calometric analysis of wood and wood components. Wood Sci Technol 1971;5:159–75.
[8] Milosavljevic I, Oja V, Suuberg EM. Thermal effects in cellulose pyrolysis: relationship to char formation processes. Ind Eng Chem Res 1996;35:654–62.
[9] Rath J, Wolfinger MG, Steiner G, Krammer G, Barontini F, Cozzani V. Heat of wood pyrolysis. Fuel 2003;82:81–91.
[10] Stenseng M, Jensen A, Dam-Johansen K. Investigation of biomass pyrolysis by thermogravimetric analysis and differential scanning calorimetry. J Anal Appl Pyrolysis 2001;58–59:765–80.
[11] Gomez C, Velo E, Barontini F, Cozzani V. Influence of secondary reactions on the heat of pyrolysis of biomass. Ind Eng Chem Res 2009;48:10222–33.
[12] Haseli Y, van Oijen JA, de Goey LPH. Modeling biomass particle pyrolysis with temperature-dependent heat of reactions. J Anal Appl Pyrolysis 2011;90:140–54.
[13] Lee CK, Chaiken RF, Singer JM. Charring pyrolysis of wood in fires by laser simulation. Symp Int Combust 1977;16:1459–70.
[14] Comesana JA, Niestroj M, Granada E, Szlek A. TG–DSC analysis of biomass heat capacity during pyrolysis process. J Energy Inst 2013. http://dx.doi.org/10.1179/1743967112Z.00000000055.
[15] Blokhin AV, Voitkevich OV, Kabo GJ, Paulechka YU, Shishonok MV, Kabo AG, et al. Thermodynamic properties of plant biomass components. Heat capacity, combustion energy, and gasification equilibria of cellulose. J Chem Eng Data 2011;56:3523–31.
[16] Harada T, Hata T, Ishihara S. Thermal constants of wood during the heating process measured with the laser flash method. J Wood Sci 1998;44:425–31.
[17] Ragland KW, Aerts DJ. Properties of wood for combustion analysis. Bioresour Technol 1991;37:161–8.
[18] Brown ME. Handbook of thermal analysis and calorimetry, principles and practice, vol. 1. Amsterdam: Elsevier; 1998.
[19] Agarwal G, Lattimer B. Method for measuring the standard heat of decomposition of materials. Thermochim Acta 2012;545:34–47.
[20] Koch P. Specific heat of ovendry spruce pine wood and bark. Wood Sci 1969;1:203–14.
[21] Green DW, Perry RH. Perry's chemical engineers' handbook. 8 ed. New York: McGraw-Hill; 2008.
[22] Hansson KM, Leckner B, Samuelsson J, Persson H, Tullin CJ. Carbon release from biomass pellets-experiments and modelling. In: Nordic seminar on small scale wood combustion 2000. Nadendal, Finland. p. 1–9.
[23] Merrick D. Mathematical models of the thermal decomposition of coal. 2. Specific heats and heats of reaction. Fuel 1983:540–6.
[24] Boutin O, Ferrer M, Lede J. Radiant flash pyrolysis of cellulose – evidence for the formation of short life time intermediate liquid species. J Anal Appl Pyrolysis 1998;47:13–31.
[25] Fisher T, Hajaligol M, Waymack B, Kellogg D. Pyrolysis behavior and kinetics of biomass derived materials. J Anal Appl Pyrolysis 2002;62:331–49.
[26] Wofinger MG, Rath J, Krammer G, Barontini F, Cozzani V. Influence of the emissivity of the sample on differential scanning calorimetry measurements. Thermochim Acta 2001;372:11–8.
[27] Basu P. Biomass gasification and pyrolysis: practical design and theory. Oxford: Elsevier; 2010.
[28] Mohan D, Pittman CU, Steele PH. Pyrolysis of wood/biomass for bio-oil: a critical review. Energy Fuels 2006;20:848–89.
[29] Mok WSL, Antal MJ. Effects of pressure on biomass pyrolysis. II. Heats of reaction of cellulose pyrolysis. Thermochim Acta 1983;68:165–86.
[30] Raveendran K, Ganesh A, Khilar KC. Pyrolysis characteristics of biomass and biomass components. Fuel 1996;75:987–98.
[31] Yang H, Yan R, Chen H, Zheng C, Lee DH, Liang DT. In-depth investigation of biomass pyrolysis based on three major components: hemicellulose, cellulose and lignin. Energy Fuels 2006;20:388–93.